

Intrinsic Proton NMR Studies of $\text{Mg}(\text{OH})_2$ and $\text{Ca}(\text{OH})_2$

Yutaka Itoh^{1*} and Masahiko Isobe²

¹Department of Physics, Graduate School of Science, Kyoto Sangyo University, Kyoto 603-8555, Japan

²Max-Planck-Institut für Festkörperforschung, Heisenbergstrasse 1, D-70569 Stuttgart, Germany

We studied the short proton free induction decay signals and the broad ^1H NMR spectra of $\text{Mg}(\text{OH})_2$ and $\text{Ca}(\text{OH})_2$ powders at 77–355 K and 42 MHz using pulsed NMR techniques. Using a Gaussian-type back extrapolation procedure for the obscured data of the proton free induction decay signals, we obtained more precise values of the second moments of the Fourier-transformed broad NMR spectra than those in a previous report [Y. Itoh and M. Isobe, J. Phys. Soc. Jpn. **84**, 113601 (2015)] and compared with the theoretical second moments. The decrease in the second moment could not account for the large decrease in the magnitude of the intrinsic proton spin-lattice relaxation rate $1/T_1$ from $\text{Mg}(\text{OH})_2$ to $\text{Ca}(\text{OH})_2$. The analysis of $1/T_1 \propto \exp(-E_g/k_B T)$ with $E_g \sim 0.01$ eV points to a local hopping mechanism, and that of $1/T_1 \propto T^n$ with $n \sim 0.5$ points to an anharmonic rattling mechanism.

1. Introduction

The divalent hydroxides of $\text{M}(\text{OH})_2$ ($\text{M} = \text{Mg}, \text{Ca}$) have a CdI_2 -type structure with broken site-symmetry at the hydrogen site. The atomic displacement parameters of the proton at the $6i$ Wyckoff site ($x, 2x, z$) in $P\bar{3}$ are large^{1,2)} and comparable to those of the rattling ions in the cage structures of pyrochlore systems.³⁾ Theoretical computer analyses indicate anharmonic motion and temperature-dependent angular correlation of the OH groups.^{4,5)}

In recent pulsed NMR experiments for $\text{Mg}(\text{OH})_2$ and $\text{Ca}(\text{OH})_2$ powders,⁶⁾ we have found that the free induction decay (FID) of the proton magnetization is a superposition of a short decay in $\sim 30 \mu\text{s}$ and a long decay in ~ 1 ms. Then, the corresponding frequency spectra show the superposition of broad and narrow components, which are assigned to intrinsic immobile protons and extrinsic mobile protons, respectively.^{6,7)}

Long before our reports, the pulsed NMR studies on proton motion showed nonexponential proton spin-lattice relaxation curves^{8,9)} and a slowing down effect for $\text{Ca}(\text{OH})_2$.⁹⁾ However, our pulsed NMR studies revealed the nonexponential relaxation of the long FIDs (narrow components in the frequency spectra) and the single/nearly single exponential relaxations of the short FIDs (broad components in the frequency spectra) for $\text{Mg}(\text{OH})_2$ and $\text{Ca}(\text{OH})_2$.^{6,7)} No slowing down effects were reproduced. The details of our NMR studies on the narrow components were reported in Ref. 7. Now, we revisit the broad components and the NMR analysis for the intrinsic proton NMR signals.

The proton dipole field is so strong causing a short FID of the proton magnetization (nuclear spin $I = 1/2$) in hydrogen compounds. In the actual pulsed NMR experiment, an obscure portion of the FID following an excitation rf pulse prevents us from obtaining the full lineshape of a Fourier-

transformed (FT) frequency spectrum because of the lack of the short-time decay. How to handle the obscured portion of the FID following the excitation pulse is an issue in Fourier analysis.¹⁰⁾ The time shifting of a single exponential FID placed at zero time leads to a Lorentzian spectrum regardless of the zero. However, a time-shifted Gaussian decay does not lead to a simple Gaussian lineshape. The dead time data of the FID also prevents us from obtaining the precise value of the second moment of the FT NMR spectrum.

In $\text{Mg}(\text{OH})_2$ and $\text{Ca}(\text{OH})_2$ powders, the short proton magnetization decays with slight oscillation.⁶⁾ Figure 1 shows the proton FID signals $F(\tau)$ for the $\text{Mg}(\text{OH})_2$ powder at 77 and 355 K, where τ is the time following an excitation rf pulse, at a Larmor frequency ν_L of 42.5772 MHz in an external magnetic field of 1.0 T. The sample preparation and characterization have been carried out in previous studies.^{6,7)} The oscilla-

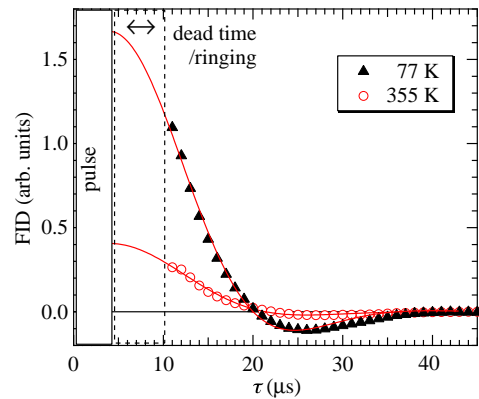


Fig. 1. (Color online) Proton free induction decay (FID) signals $F(\tau)$ for $\text{Mg}(\text{OH})_2$ powder at 77 and 355 K. The length of an excitation rf pulse is 4 μs . The FID below 10 μs is obscured. Solid curves are the results from the least-squares fitting using an analytical function given by Eq. (1).

*E-mail: yitoh@cc.kyoto-su.ac.jp

tion is a Lowe beat in the FID due to a nuclear dipole–dipole interaction.¹¹⁾ The oscillating decay can be traced back to the magnetic dipolar lineshape of a more rectangular type than a Gaussian type.¹²⁾ The short part of the FID ($\tau < 10 \mu\text{s}$) is obscured by probe ringing and/or dead time. Since the decay time of the FID is typically $\sim 30 \mu\text{s}$, the time shifting of an FID placed at zero time may lead to a spurious FT spectrum.

Although a solid echo can be helpful for determining zero time of FID signals for dipolar-coupled systems,¹³⁾ a recent analysis using a Gaussian back-extrapolation procedure for the obscured FID provides us with an alternative convenient method.¹⁰⁾ The NMR spectrum from the composite FID is confirmed to be nearly identical to the magic-echo spectrum for some hydrides,¹⁰⁾ and then the extrapolation procedure has been applied to various hydrogen compounds.^{14–17)}

In this paper, we adopted a replacement procedure to analyze the proton FID for $\text{Mg}(\text{OH})_2$ and $\text{Ca}(\text{OH})_2$, which made the FT-NMR analysis better than that in a previous report.⁶⁾ The portion of the FID obscured by probe ringing and/or dead time was replaced by the extrapolated data using an analytical fitting function. We report the detailed analysis of the FID and the broad components (intrinsic protons) in the NMR spectra for $\text{Mg}(\text{OH})_2$ and $\text{Ca}(\text{OH})_2$ powders, and discuss possible relaxation mechanisms of the intrinsic proton spin-lattice relaxation rate $1/T_1$.

2. FID Analysis

The observable part of the FID was extrapolated back to zero time using an analytical decay function, which joined the extrapolated data to the part not obscured by probe ringing and/or dead time. Then, the resulting composite FIDs were analyzed by Fourier transformation.

We adopted the following modulated Gaussian function,¹²⁾

$$F(\tau) = F(0)\exp\left[-\frac{a^2\tau^2}{2}\right]\frac{\sin b\tau}{b\tau}, \quad (1)$$

where $F(0)$, a , and b are fitting parameters. The second moment M_2 of the frequency spectrum is given by

$$M_2 = a^2 + \frac{1}{3}b^2, \quad (2)$$

and the half-width of the frequency spectrum is given by

$$\Delta\nu = \sqrt{M_2}. \quad (3)$$

In Fig. 1, the solid curves are the results from the least-squares fitting using an analytical function given by Eq. (1) for $\tau < 40 \mu\text{s}$. Figure 2 shows the temperature dependences of the decay rates a and b for the short FID, and the half-width $\Delta\nu$ for NMR spectra in $\text{Mg}(\text{OH})_2$ (left) and $\text{Ca}(\text{OH})_2$ (right). Open symbols are the theoretical values estimated from Van Vleck's second moment formula for the homonuclear dipole coupling on a rigid lattice. The lattice constants and the site parameters in the neutron diffraction data were adopted for the estimation.^{1,2)}

The temperature dependence of a in $\text{Mg}(\text{OH})_2$ is different from that in $\text{Ca}(\text{OH})_2$. One should note that a and b are phe-

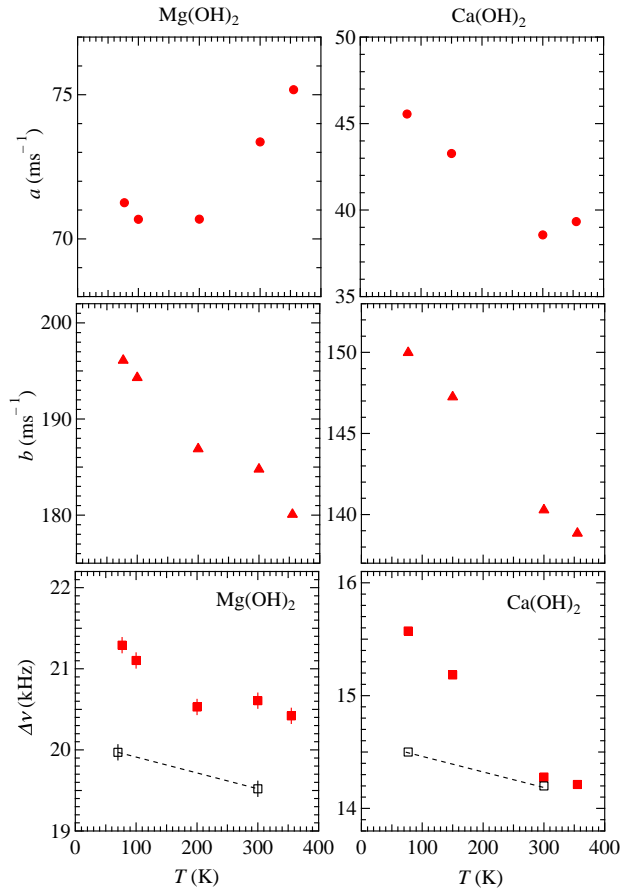


Fig. 2. (Color online) Temperature dependences of decay rates of a , b , and a half-width $\Delta\nu$ for broad NMR spectra at $\nu_L = 42.5772$ MHz in $\text{Mg}(\text{OH})_2$ (left) and $\text{Ca}(\text{OH})_2$ (right). Open symbols are the theoretical values estimated from the rigid-lattice dipole fields through Van Vleck's second moment formula. The dashed lines are visual guides.

nomenological parameters in the second moment of Eq. (2).¹²⁾ Then, we have no theoretical accounts for the difference.

The experimental half-widths $\Delta\nu$'s of $\text{Ca}(\text{OH})_2$ are about 0.7 times those of $\text{Mg}(\text{OH})_2$. This is reasonable, because the lattice constants of $\text{Ca}(\text{OH})_2$ are longer than those of $\text{Mg}(\text{OH})_2$.^{1,2)} Qualitatively, the lattice expansion through Van Vleck's formula reproduces the decrease in $\Delta\nu$ from $\text{Mg}(\text{OH})_2$ to $\text{Ca}(\text{OH})_2$. In Fig. 2, however, the experimental $\Delta\nu$ (closed symbols) of $\text{Ca}(\text{OH})_2$ more steeply decreases with heating than the theoretical $\Delta\nu$ (open squares) on the rigid lattice.

The obscured parts of the short FIDs below $10 \mu\text{s}$ in Fig. 1 were replaced by fitting Eq. (1) to the unobscured data. Figure 3 shows the FT-NMR spectra of the extrapolated FIDs for $\text{Mg}(\text{OH})_2$ and $\text{Ca}(\text{OH})_2$ at 355 K and $\nu_L = 42.5772$ MHz. NMR spectra consist of broad and narrow components, which were assigned to intrinsic (immobile) and extrinsic (mobile) protons, respectively.⁶⁾ The narrow spectra come from the long FIDs ($60 \mu\text{s} < \tau < 2$ ms),⁷⁾ which are out of the frame of

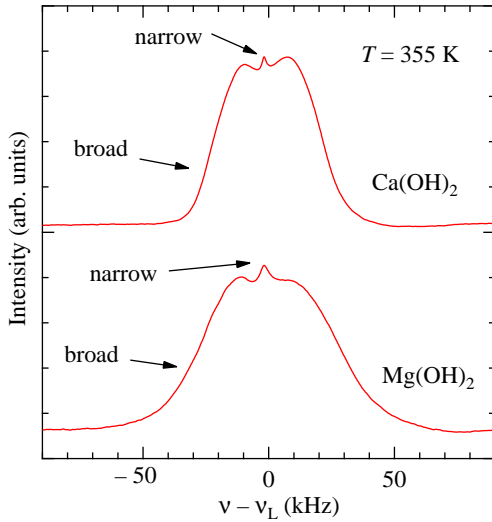


Fig. 3. (Color online) FT-NMR spectra for $\text{Mg}(\text{OH})_2$ and $\text{Ca}(\text{OH})_2$ at 355 K and $\nu_L = 42.5772$ MHz. NMR spectra consist of broad and narrow components, which are assigned to intrinsic (immobile) and extrinsic (mobile) protons, respectively. The broad components are of rectangular type rather than Gaussian.

Fig. 1. The broad components of the pulsed FT-NMR spectra are compatible with the NMR absorption spectra measured by the continuous-wave method.^{18–20} Not simple Gaussian but rectangular-type line shapes characterize the broad components. The intensities of the broad components relative to the narrow ones were underestimated in the original analysis⁶ and were properly corrected in a previous report.⁷

3. Proton Spin-Lattice Relaxation Rates of Broad Components

Figure 4 shows the temperature dependences of the intrinsic proton spin-lattice relaxation rates $1/T_1$'s (upper panel) and $1/T_1T$'s (lower panel) of the broad components for $\text{Mg}(\text{OH})_2$ and $\text{Ca}(\text{OH})_2$, which are reproduced from previous reports.^{6,7} The temperature dependence of $1/T_1$ for $\text{Ca}(\text{OH})_2$ is parallel to that below 200 K in Ref. 9.

The concentration of a hypothetical impurity spin-1/2 was estimated to be at most 99 ppm for $\text{Mg}(\text{OH})_2$ and 56 ppm for $\text{Ca}(\text{OH})_2$ from Curie magnetism in the bulk magnetic susceptibility.²¹ The NMR measurement is a touchstone to test whether the impurity is substituted or mixed. Finite effects of the dilute magnetic impurities on the relaxation rates are excluded, because all the proton magnetizations in the broad component recover with a single exponential function for $\text{Mg}(\text{OH})_2$.⁶ The stretched exponential relaxation with the variable exponent β of ~ 0.9 for $\text{Ca}(\text{OH})_2$ may be due to some impurity effect.⁷ However, the fact that T_1 for $\text{Ca}(\text{OH})_2$ is about 10 times longer than that for $\text{Mg}(\text{OH})_2$ is in contrast to the impurity effect.

The magnitude of $1/T_1$ for $\text{Ca}(\text{OH})_2$ is about 0.1 times that for $\text{Mg}(\text{OH})_2$. Both $1/T_1T$'s monotonically decrease as tem-

perature increases. This is in contrast to the conventional Raman scattering of acoustic phonons, by which $1/T_1T$ increases as temperature increases.¹²

In general, the proton spin-lattice relaxation rate $1/T_1$ is proportional to the coupling constant of $(\Delta\nu)^2$ (second moment).^{12,22,23} $\Delta\nu$ for $\text{Ca}(\text{OH})_2$ is about 0.7 times that for $\text{Mg}(\text{OH})_2$. Only the decrease of 0.49 in the coupling constant of $(\Delta\nu)^2$ is insufficient to account for the large decrease of 0.1 in $1/T_1$.

The higher atomic mass of the Ca ion than that of the Mg ion and the lattice expansion from $\text{Mg}(\text{OH})_2$ to $\text{Ca}(\text{OH})_2$ cause frequency shifts in lattice vibration modes, which in optical phonons were observed by Raman spectroscopy.²⁴ The lattice expansion is also expected to lead to the lower Debye frequency of $\text{Ca}(\text{OH})_2$ than that of $\text{Mg}(\text{OH})_2$. The Raman scattering of acoustic phonons leads to $1/T_1 \propto (\Delta\nu)^2 \Theta_D T^2$ with a Debye cut-off frequency of $\Theta_D \sim a_H^{-1}$ (a_H is the nearest-neighbor proton-proton distance).¹² We estimated the decrease of ~ 0.4 in $(\Delta\nu)^2 \Theta_D$ from $\text{Mg}(\text{OH})_2$ to $\text{Ca}(\text{OH})_2$, which is insufficient to reproduce the decrease in 0.1 in $1/T_1$.

Figure 5(a) shows semilog plots of T_1 's against $10^3/T$. Solid lines are the results from the least-squares fitting using a thermal activation function of $T_1 = C \exp(E_g/k_B T)$ with the fitting parameters C and E_g . We estimated the activation energies of $E_g = 0.011$ eV for $\text{Mg}(\text{OH})_2$ and 0.012 eV for $\text{Ca}(\text{OH})_2$. These values are smaller than the previous NMR estimation of 0.21 eV for $\text{Ca}(\text{OH})_2$,⁹ the activation energy of

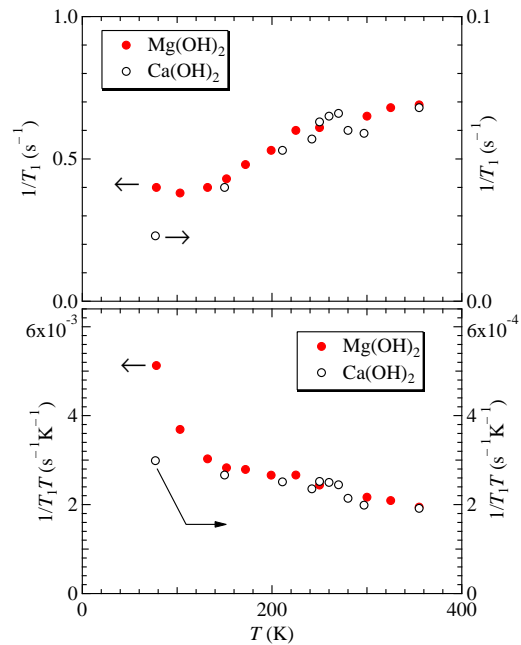


Fig. 4. (Color online) Temperature dependences of the intrinsic proton spin-lattice relaxation rates $1/T_1$'s (upper panel) and $1/T_1T$'s (lower panel) at 42.5772 MHz for $\text{Mg}(\text{OH})_2$ and $\text{Ca}(\text{OH})_2$ powders, which are reproduced from previous reports.^{6,7} The magnitude of $1/T_1$ for $\text{Ca}(\text{OH})_2$ is about 0.1 times that for $\text{Mg}(\text{OH})_2$.

2.0 eV for the proton conductivity,²⁵⁾ and the excitation energy of 0.4 eV for a proton jump in a local Morse potential.²⁶⁾ The energy E_g may be the local hopping energy of the proton over three equivalent positions at the $6i$ Wyckoff site ($x, 2x, z$) in $P\bar{3}$.

Figure 5(b) shows log–log plots of $1/T_1$'s against temperature. The solid lines are the results from the least-squares fitting using a power-law function of $1/T_1 = AT^n$ with the fitting parameters A and n . We estimated the powers of $n = 0.54$ for $\text{Mg}(\text{OH})_2$ and 0.64 for $\text{Ca}(\text{OH})_2$, which are inconsistent with $n = 2$ of the two-phonon Raman scattering of acoustic phonons.¹²⁾ The powers of $n = 0.54$ and 0.64 remind us of $1/T_1 \propto \sqrt{T}$ due to dilute electron gas in semiconductors¹²⁾ and due to rattling phonons.²⁷⁾

In $\text{Mg}(\text{OH})_2$ and $\text{Ca}(\text{OH})_2$, dilute mobile protons with Boltzmann statistics may act as the scattering carriers to the immobile protons. However, the dc conductivity of $\text{Ca}(\text{OH})_2$ is much higher than that of $\text{Mg}(\text{OH})_2$.²⁵⁾ Since the carrier density n_H is in $1/T_1 \propto n_H \sqrt{T}$,¹²⁾ if $\text{Ca}(\text{OH})_2$ involves a higher carrier density than $\text{Mg}(\text{OH})_2$, the $1/T_1$ of $\text{Ca}(\text{OH})_2$ would be higher than that of $\text{Mg}(\text{OH})_2$. However, this is in contrast to

the experimental results.

Finally, we consider the effect of the anharmonic motion of the hydroxyl group due to broken site-symmetry.^{1,2,4,5)} The neutron diffraction experiments indicate the large atomic displacement parameters of the protons,^{1,2)} which are similar to those of the rattling ions in the pyrochlore.³⁾ The anharmonic motion of the proton at the $6i$ Wyckoff site ($x, 2x, z$) in $P\bar{3}$ can play a role in $1/T_1 \propto \sqrt{T}$ in the same way as the rattling phonons in the pyrochlore systems.²⁷⁾

4. Conclusions

We analyzed the proton FIDs for $\text{Mg}(\text{OH})_2$ and $\text{Ca}(\text{OH})_2$ powders using an extrapolation function to the obscured parts of FIDs, estimated the second moments of the intrinsic proton NMR spectra, and obtained the rectangular-type broad FT-NMR spectra. We found a large decrease in the magnitude of the intrinsic proton spin-lattice relaxation rate $1/T_1$ from $\text{Mg}(\text{OH})_2$ to $\text{Ca}(\text{OH})_2$, which the decrease in the second moment is insufficient to account for. Local hopping and anharmonic rattling motions of the proton are the promising candidates for the proton spin-lattice relaxation mechanism.

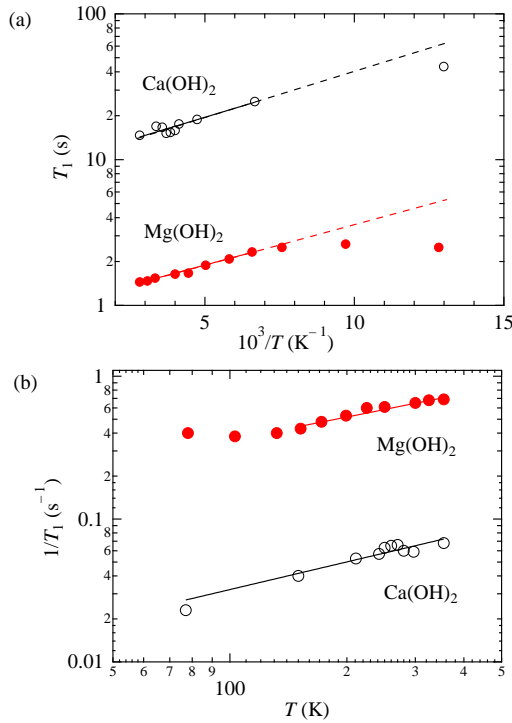


Fig. 5. (Color online) (a) Semilog plots of the intrinsic proton spin-lattice relaxation times T_1 's against $10^3/T$ for $\text{Mg}(\text{OH})_2$ and $\text{Ca}(\text{OH})_2$.^{6,7)} Solid lines are the results from the least-squares fitting using a thermal activation function of $T_1 = C \exp(E_g/k_B T)$: $E_g = 0.011$ eV for $\text{Mg}(\text{OH})_2$ and 0.012 eV for $\text{Ca}(\text{OH})_2$. Dashed lines are visual guides. (b) Log–log plots of the intrinsic proton spin-lattice relaxation rates $1/T_1$'s against temperature for $\text{Mg}(\text{OH})_2$ and $\text{Ca}(\text{OH})_2$.^{6,7)} Solid lines are the results from the least-squares fitting using a power-law function of $1/T_1 = AT^n$: $n = 0.54$ for $\text{Mg}(\text{OH})_2$ and 0.64 for $\text{Ca}(\text{OH})_2$.

- 1) L. Desgranges, G. Calvarin, and G. Chevrier, *Acta Crystallogr., Sect. B* **52**, 82 (1996).
- 2) L. Desgranges, D. Grebille, G. Calvarin, G. Chevrier, N. Floquet, and J.-C. Niepce, *Acta Crystallogr., Sect. B* **49**, 812 (1993).
- 3) Z. Hiroi, J. Yamaura, and K. Hattori, *J. Phys. Soc. Jpn.* **81**, 011012 (2012).
- 4) P. T. Jochym, A. M. Oles, K. Parlinski, J. Lazewski, P. Piekarczyk, and M. Sternik, *J. Phys.: Condens. Matter* **22**, 445403 (2010).
- 5) S. Raugé, P. L. Silvestrelli, and M. Parrinello, *Phys. Rev. Lett.* **83**, 2222 (1999).
- 6) Y. Itoh and M. Isobe, *J. Phys. Soc. Jpn.* **84**, 113601 (2015).
- 7) Y. Itoh and M. Isobe, *J. Phys. Soc. Jpn.* **85**, 034602 (2016).
- 8) R. E. J. Sears, R. Kaliaperumal, and S. Manogaran, *J. Chem. Phys.* **88**, 2284 (1988).
- 9) J. A. Moreno, S. Mizrachi, and V. Oppeltz, *Solid State Commun.* **51**, 597 (1984).
- 10) S. K. Brady, M. S. Conradi, G. Majer, and R. G. Barnes, *Phys. Rev. B* **72**, 214111 (2005).
- 11) I. J. Lowe and R. E. Norberg, *Phys. Rev.* **107**, 46 (1957).
- 12) A. Abragam, *Principles of Nuclear Magnetism* (Oxford University Press, Oxford, 1961) pp. 120, 390, 407.
- 13) C. P. Slichter, *Principles of Magnetic Resonance* (Springer-Verlag, Tokyo, 1996) p. 371.
- 14) R. L. Corey, T. M. Ivancic, D. T. Shane, E. A. Carl, R. C. Bowman, Jr., J. M. Bellosta von Colbe, M. Dornheim, R. Bormann, J. Huot, R. Zidan, A. C. Stowe, and M. S. Conradi, *J. Phys. Chem. C* **112**, 19784 (2008).
- 15) D. T. Shane, R. L. Corey, R. C. Bowman, Jr., R. Zidan, A. C. Stowe, S.-J. Hwang, C. Kim, and M. S. Conradi, *J. Phys. Chem. C* **113**, 18414 (2009).
- 16) D. T. Shane, R. L. Corey, C. McIntosh, L. H. Rayhel, R. C. Bowman, Jr., J. J. Vajo, A. F. Gross, and M. S. Conradi, *J. Phys. Chem. C* **114**, 4008 (2010).
- 17) E. G. Sorte, R. L. Corey, R. C. Bowman, Jr., D. Birkmire, R. Zidan, and M. S. Conradi, *J. Phys. Chem. C* **116**, 18649 (2012).
- 18) D. D. Elleman and D. Williams, *J. Chem. Phys.* **25**, 742 (1956).
- 19) D. M. Henderson and H. S. Gutowsky, *Am. Mineral.* **47**, 1231 (1962).
- 20) F. Holuj and J. Wiczorek, *Can. J. Phys.* **55**, 654 (1977).
- 21) A superconducting quantum interference device (SQUID) magnetometer was used to measure the bulk magnetic susceptibility for the present $\text{Mg}(\text{OH})_2$ and $\text{Ca}(\text{OH})_2$ powder in an external magnetic field of 1 T.

- 22) N. Bloembergen, E. M. Purcell, and R. V. Pound: Phys. Rev. **73**, 679 (1948).
- 23) T. Moriya, Prog. Theor. Phys. **16**, 641 (1956).
- 24) P. Dawson, C. D. Hadfield, and G. R. Wilkinson, J. Phys. Chem. Solids **34**, 1217 (1973).
- 25) F. Freund and H. Wengeler, Ber. Bunsenges. Phys. Chem. **84**, 866 (1980).
- 26) F. Freund, in *Proton Conductors*, ed. P. Colomban (Cambridge University Press, Cambridge, 1992) p. 138.
- 27) T. Dahm and K. Ueda, J. Phys. Chem. Solids **69**, 3160 (2008).